Impact of potentially toxic elements on pines in a former ore processing mine :

Luc Béraud, Arnaud Elger, Thomas Rivière, Olivier Berseille, Philippe Déliot, Jérôme Silvestre, Camille Larue, Laurent Poutier, Sophie Fabre

Environmental Research 227 (2023) 115747

Contents lists available at ScienceDirect

Environmental Research

journal homepage: www.elsevier.com/locate/envres

Impact of potentially toxic elements on pines in a former ore processing mine: Exploitation of hyperspectral response from needle and canopy scales

Luc Béraud [a,b], Arnaud Elger [b], Thomas Rivière [a], Olivier Berseille [b], Philippe Déliot [a], Jérôme Silvestre [b], Camille Larue [b], Laurent Poutier [a], Sophie Fabre [a,*]

[a] Office National d'Études et de Recherches Aérospatiales (ONERA), Toulouse, France
[b] Laboratoire Ecologie Fonctionnelle et Environnement, Université de Toulouse, CNRS, Toulouse, France

ARTICLE INFO

Handling Editor: Aijie Wang

Keywords:
Soil contamination
Vegetation monitoring
Hyperspectral
Spectral index
Regression
Airborne imagery

ABSTRACT

Anthropic potentially toxic element (PTE) releases can lead to persistent pollution in soil. Monitoring PTEs by their detection and quantification on large scale is of great interest. The vegetation exposed to PTEs can exhibit a reduction of physiological activities, structural damage … Such vegetation trait changes impact the spectral signature in the reflective domain 0.4–2.5 μm. The objective of this study is to characterize the impact of PTEs on the spectral signature of two pine species (Aleppo and Stone pines) in the reflective domain and ensure their assessment. The study focuses on nine PTEs: As, Cr, Cu, Fe, Mn, Mo, Ni, Pb, Zn. The spectra are measured by an in-field spectrometer and an aerial hyperspectral instrument on a former ore processing site. They are completed by measurements related to vegetation traits at needle and tree scales (photosynthetic pigments, dry matter, morphometry …) to define the most sensitive vegetation parameter to each PTE in soil. A result of this study is that chlorophylls and carotenoids are the most correlated to PTE contents. Context-specific spectral indices are specified and used to assess metal contents in soil by regression. These new vegetation indices are compared at needle and canopy scales to literature indices. Most of the PTE contents are predicted at both scales with Pearson correlation scores between 0.6 and 0.9, depending on species and scale.

1. Introduction

Potentially toxic elements (PTEs), released by various anthropic activities like mining, smelting or other industrial activities, can lead to persistent pollution in soil even after the exploitation has ceased. The environment is then exposed to the transfer and dissemination of PTEs causing water and soil contamination and loss of biodiversity. Currently, environmental monitoring mainly depends on traditional geochemical methods using, for example, *in-situ* measurements with portable XRF (X-Ray Fluorescence) devices completed by laboratory analysis of soil samples (Lemière, 2018; Parsons et al., 2013). These methods are time-consuming and unsuitable for large-scale monitoring. Therefore, monitoring PTEs (i.e. detecting and quantifying them) on large scale for various land covers (from bare soil to dense vegetation) is of great interest and can be achieved by remote sensing (Ong et al., 2019).

Vegetation exposed to PTEs can exhibit a modification of physiological activities (revealed e.g. by pigment concentrations) and structural damage at leaf and canopy scales (Küpper and Andresen, 2016; Slonecker et al., 2010; Zhou et al., 2018). Such changes in vegetation traits impact the spectral signature in the reflective domain [400–2500 nm]. Passive optical remote sensing devices, in particular hyperspectral ones, have been widely used to assess these vegetation traits (Blackburn, 2007; Homolová et al., 2013; Kokaly et al., 2009; Lausch et al., 2016). The information contained in the optical hyperspectral signal is then exploited via two types of approaches (Verrelst et al., 2019; Zhang et al., 2021): machine learning regression methods based on the empirical relationship between spectral variables (e.g. spectral signatures or transformations: continuum removal, spectral indices, first derivate) and vegetation traits like pigment concentrations (Peng et al., 2018; Verrelst et al., 2012) or numerical inversion of physically-based leaf and canopy Radiative Transfer Models (RTM) (Feret et al., 2019; Lassalle et al., 2019a; Li et al., 2019). Some hybrid regression methods combine RTM simulations with machine learning regression methods (Verrelst et al., 2019).

PTE pollution can have a minor impact and be species-dependent according to their sensitivity to particular PTEs. Coniferous species are very common and widespread in European forests. Pines were noted to

* Corresponding author. ONERA DOTA BP74025 2 av. Edouard Belin, FR-31055, Toulouse, Cedex 4, France.
E-mail address: sophie.fabre@onera.fr (S. Fabre).

https://doi.org/10.1016/j.envres.2023.115747
Received 16 December 2022; Received in revised form 11 March 2023; Accepted 22 March 2023
Available online 24 March 2023

Main abbreviations

DBH	Diameter at Breast Height
NIR	Near-Infrared
PTE	Potentially Toxic Element
SWIR	Short-Wave Infrared
VI	Vegetation Indices
VIS	Visible

be sensitive to PTEs (Shin et al., 2019). The measurement of optical properties of coniferous needles is known to be difficult, due to their geometry, and is underrepresented in published reports compared to broadleaves (Mõttus et al., 2017; Rautiainen et al., 2018).

The PTE effects are also combined with other natural or environmental stressors of greater impact, such as drought, poor soil quality or surface runoff (Gamon et al., 2019; Moor et al., 2017). The retrieval of PTE effects on vegetation by hyperspectral data is challenging and site-specific (Wang et al., 2018).

To reduce environmental stressor impact and achieve sensitive species inventory, PTE effects on vegetation spectral signature can be first studied at leaf or canopy scales before upscaling to airborne or satellite levels (Lassalle et al., 2019b, 2021). The accuracy of prediction may then be reduced when transposed to canopy scale, with the increasing influence of background signal, mixed pixels and canopy structure (Rautiainen et al., 2018). Several studies have assessed the ability of field spectrometers to retrieve in-field foliar PTE contents, including pine needles, or soil PTE contents in vegetated lands (Mirzaei et al., 2019; Shin et al., 2019; Zhou et al., 2018).

For various plant species (white birch, Mongolian oak, grapevine - *Vitis vinifera cv. Askari*, rice - *Oriza sativa* L., cotton grass), many studies proposed approaches coupling optimized or existing spectral vegetation indices applied to *in-situ* spectral measurements and multiple regressions to explore the relation with PTE contents (such as As, Cd, Co, Cr, Cu, Zn, Pb, Mo, and Ni) in leaves (Bandaru et al., 2016; Lassalle et al., 2021; Mirzaei et al., 2019; Zhou et al., 2018). They found a determination coefficient ranging from 0.43 to 0.84 between estimated and measured foliar PTE contents. Some studies dealt with the relation between vegetation reflectances at specific spectral bands and PTE contents in soil without assessment of foliar PTE contents. Shi et al. demonstrated that two indices from the literature in the VISible (VIS)-Near InfraRed (NIR) spectral domain (400–900 nm), PRI (Photochemical Reflectance Index) and REP (Red Edge Position) may be used as vegetation indices to monitor arsenic contamination in agricultural soils planted with rice (*Oryza sativa* L.) (Shi et al., 2016). They retained three spectral bands (552, 568 and 716 nm) to build an optimized spectral index. Mirzaei et al. identified the most sensitive wavelengths in the VIS-NIR domains for the estimation of Cu, Zn, Pb, Cr, and Cd contents in the grapevine (*Vitis vinifera cv. Askari*) leaves (Mirzaei et al., 2019). Shin et al. (2019) demonstrated the correlation between the first derivatives of needle spectral signatures at 668 nm and 1648 nm and As contents in needles and soil (determination coefficient between As contents in pine needles and soil samples of 0.79). This study was however based on needles of a unique pine species *P. densiflora* and a single PTE, As, while metal contamination in soils is usually polymetallic (Doumas et al., 2018).

Few studies go through airborne remote sensing for detecting and characterizing PTE soil contamination in vegetated areas. Airborne hyperspectral imagery in VIS-NIR spectral domain was used to map leaf metal contents (Cr, Cu, Ni and Zn) of the species Rubus fruticosus L. over industrial brownfields (Lassalle et al., 2021). Optimized normalized vegetation indices, exploiting pigment-related wavelengths, were specified and allowed the prediction of metal contents with good accuracy in the field and on the image, especially Cu and Zn ($r \geq 0.84$). This study however concerned a single species, the bramble (Rubus fruticosus L.), and four PTEs. Another study provided good accuracy to detect plants affected by several soil PTE (As, Cr, Cu, Sn and Zn) in mining area from airborne hyperspectral imagery and Random Forest algorithm (Yang et al., 2020).

Most of the published studies were limited to in-field spectral measurements without addressing airborne measurements and have focused on the spectral range [400–900 nm] not considering the spectral bands beyond 1000 nm. Few studies concerned pine species, a priori sensitive to PTEs in soil, and polymetallic contamination by various metals and metalloids. To our knowledge, there is no published study based on a comprehensive database construction (including spectral measurements, soil metal contents, biophysical, biochemical and structural traits) to identify pine species traits altered by chemical contamination.

The objective of our study was to assess PTE contents in soil by the spectral signature of two pine species in the reflective spectral domain [400–2500 nm] measured by an airborne hyperspectral instrument. This study focused on nine PTEs: As, Cr, Cu, Fe, Mn, Mo, Ni, Pb, Zn. The studied contaminated land is a former ore processing site which has been phytostabilized for several years (§ 2.1). A complete database was built with needle-scale spectral signatures measured during an *in-situ* experiment completed by soil PTE contents, foliar pigment contents and other biophysical vegetation traits at needle and tree scales (§ 2.2 and 2.3). This database allowed to define the most sensitive vegetation parameters to each soil PTE and to select the best suited wavelengths establishing context-specific spectral indices. Those indices were used by an empirical approach to assess the sensitive vegetation parameters and soil PTE contents by regression (§ 2.5). They were compared to indices provided in the literature. Finally, the performance of the proposed approach was assessed on the hyperspectral image, at the canopy scale (§ 3). The behaviours of two pine species were compared in order to identify the most sensitive one and to analyse behaviour similarities and differences in this contaminated context (§ 4).

2. Materials and methods

2.1. Study site

The site is a former ore processing site under a Submediterranean climate located in Southern France closed in 2004 and managed by an operator of the French public body. This site has been phytostabilized in 2006 to avoid the mobility of PTEs in soil, and natural vegetation has grown over the years (Fig. 1) (Fabre et al., 2020). The control pines are located 2–3 km from the contaminated area in the opposite direction of the prevailing winds to avoid the potential deposition of PTEs. Studied

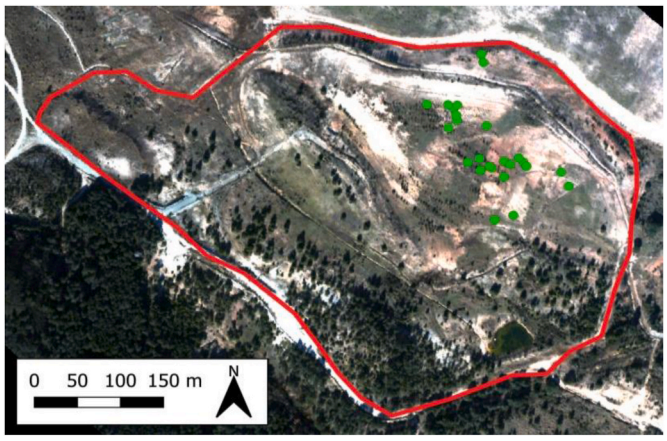

Fig. 1. Former ore processing site. The image was extracted from the RGB representation of the hyperspectral image (spatial resolution: 0.75 m). The area of interest is delineated in the red line (19.4 ha). The 26 pines of the contaminated area are in green dots.

PTEs were contained in the original ore or used in the extraction process.

Two pine species (Aleppo- *Pinus halepensis*, Stone- *Pinus pinea*) were selected for this study (Fig. 2). These species are mostly naturally established in the surrounding area, and they have been introduced into the contaminated land during the phytostabilisation process. The tree crown size range allows the monitoring of these species by airborne remote sensing.

26 pines (13 pines of each species) and 9 pines (5 Aleppo and 4 Stone pines) were sampled in the contaminated and control areas respectively (Fig. 2). The trees within the contaminated area were of comparable ages (about 15 years), and control pines were of variable ages estimated from 12 to 35 years. Their geographical coordinates were acquired using a differential GNSS.

Needle samples from contaminated and control sites have been measured in situ (structural traits, spectral signatures) and in laboratory (pigment concentrations, biophysical traits). These measurements were completed by soil PTE contents. All these soil and vegetation measurements have filled out an exhaustive database.

2.2. Soil measurements

Under each pine, the upper soil layer (0–10 cm) was sampled at about 40 cm of the trunk with a plastic shovel, deposited in a hermetic bag, and analysed for measuring PTE contents (9 elements). Also, three *in-situ* sampling replicates have been collected in opposite directions of the trunk for nine pines covering the whole contamination range, to analyse the spatial variability around the trunks. Each collected soil sample was then divided into three subsamples after quartering and then dried in an oven for 24 h at 105 °C. The particles smaller than 2 mm after passing through a nylon sieve were retained for analysis. Each subsample was split into three capsules (0.7–1 cm soil thickness) and then measured with a portable X-ray fluorescence elemental analyser (NITON XL3t GOLDD 900Analyzer, Thermo Scientific). Each sampling spot was then measured 3 × 3 times and the average PTE contents were retained as the final values. The nine elements are represented in Fig. 3a. Several elements are correlated with each other (Fig. 3b): Cu and As (Pearson r = 0.90); Ni, Mo, Fe and Mn (r > 0.77); Pb and Zn (r = 0.81). Measurements were controlled with certified reference materials of soil (BCR 141R, BCR 142R, BCR 145R, STSD3, LKSD3, IAEA SL1, WQB-1). For the 9 selected elements, the median recovery rates ranged from 89% to 124%, except for Ni which was 49%. The discrepancy for Ni could come from an overlapping band with Cu (Ran et al., 2014), and the reference contents were well retrieved.

The soil PTE contents of the three soil replicates sampled for nine pines to inform on the spatial variability were quite homogeneous around each pine. The coefficient of variation of each PTE content ranged from 0.01 to 1.02, with median values from 0.14 to 0.36 for each PTE. The median variation range at each pine covered 11%–25% of the total range of PTE soil contents.

2.3. Vegetation measurements

Measurements were achieved for 13 Aleppo and 15 Stone pines in the contaminated and control lands on 24 February 2021. Seven pines in the contaminated area (§ 2.1, Fig. 1) were not sampled during the field campaign but introduced to analyse the results at the airborne scale.

For each pine, needles were randomly sampled within the crown according to the study of Lhotáková et al. (2007). This study concluded that a random sampling of similar-aged needles within the crown might be used to study biochemical and spectral needle properties of a mature Norway spruce.

2.3.1. Biophysical and biochemical parameters

Needle samples were collected on each pine during the field experiment. Needle pigments were extracted in methanol adapting the protocol of Diepens et al. (2017) and analysed by High Performance Liquid Chromatography (HPLC). Needles were stored at −80 °C after sampling, and then randomly subsampled for pigment analysis. Three subsamples per pine sample were processed for repetition. The selected needles were freeze-dried for 24 h in the dark to prevent light degradation. The needles were then ground in a mortar with liquid nitrogen in a dark room. The pigment extraction was done with approximatively 100 mg of ground needles with a solution of 1.5 ml of methanol buffered with 2% ammonium acetate. The solution was vortexed for 1 min inside a glass ball and with short breaks every 10 s then, let still for 15 min at −20 °C. The solution was finally filtered with a 2 μm syringe filter after centrifugation (5 min, 4000 rpm at 4 °C). The extraction was done twice with the same needle material; and filtered extractions were pooled together and stored at −80 °C before the HPLC analysis. The HPLC analysis was made on an Agilent LC1200 Series system (Diepens et al., 2017) (G1315B Diode Array Detector, G1316A column compartment, G1311A pump, G1329A sampler) at 440 nm (chlorophyll *b*, carotenoids) and 665 nm (chlorophyll *a*), following the parameters of Barlow et al. (1997). Pigments were quantified with a calibrated, peak-area chromatogram analysis (Diepens et al., 2017). The pigment concentrations are expressed on the dry mass. The concentrations obtained with the three repetitions were averaged. The chlorophyll concentration was calculated with chlorophyll *a* and *b* measurements, and the carotenoid concentration was composed of β-carotene, lutein and antheraxanthin (Diepens et al., 2017). The Pearson correlation coefficient value between chlorophylls and carotenoids was 0.97.

The water contents were the averages of five mass change measurements. Five batches of five pairs of needles for each pine were randomly selected. The mass of the batch was measured before and after

Fig. 2. Studied species (a) Aleppo pine, (b) Stone pine.

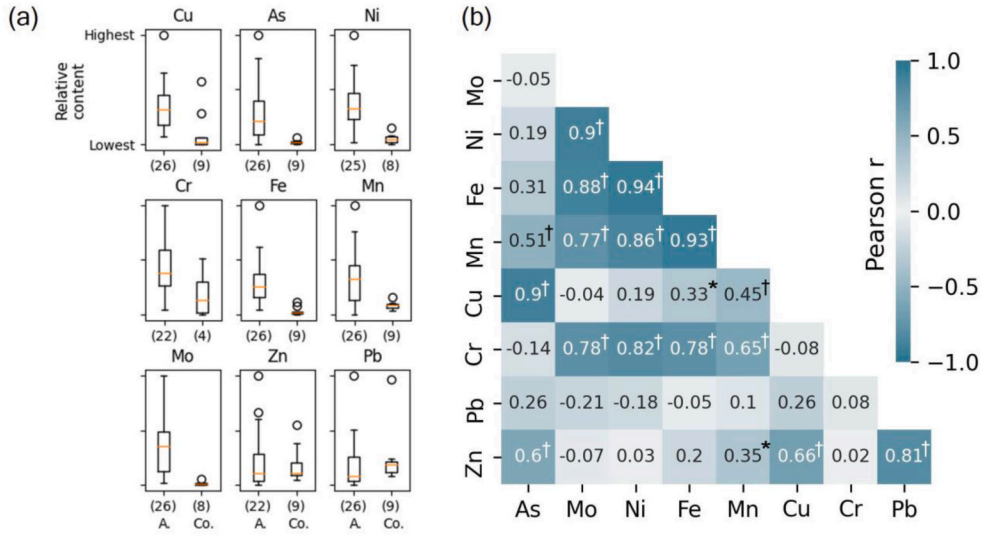

Fig. 3. (a) Relative contents of the nine PTEs, normalized for confidentiality. A.: study Area, Co.: Control area, the number of samples in each boxplot is given in brackets. (b) Pearson correlation coefficient values between PTEs. *value significant at a level of 0.05; † value significant at a level of 0.01.

oven drying for 24 h at 105 °C.

The main statistics of all these parameters for each species and each area are represented in Table S1, in the Supplementary materials.

2.3.2. Structural parameters

Even if passive optical instruments are not the best devices to give access to tree structural traits (height, Diameter at Breast Height-DBH) in comparison to LiDAR (Light Detection and Ranging) devices, canopy and foliage structure impact the spectral signature in the reflective domain. Structural traits, provided in Table 1, have been measured in situ at the individual tree level. We did not use the height and DBH measurements of three control pines, estimated to be more than 20 years old from historical aerial photographs, because of the high age difference with the pines in the contaminated area. The main statistics of all these parameters are provided in Table S1, in the Supplementary materials.

2.3.3. Spectral signatures

In-situ spectral reflectances of pine needles were acquired with an ASD FieldSpec Pro spectrometer in the [350–2500 nm] domain (Malvern Panalytical, Malvern, UK). A protocol of spectral measurements specific to pine needles was defined beforehand to make the measurement completely reproducible from one sample to another. Measurements were performed with a contact probe device. They were acquired in radiance units and converted to reflectances according to the procedure detailed in (Lesaignoux et al., 2013). All spectral signatures were then resampled to the spectral resolution of the airborne image and the same band removal and smoothing procedures (atmospheric transmittance <80% and Savitzky-Golay smoothing filter) were applied (Erudel et al., 2017) (§ 2.4).

2.4. Hyperspectral airborne image

The airborne hyperspectral image was acquired on February 13, 2019 at 13:00 UT under clear sky conditions with the AISA FENIX-1K camera system. This push-broom camera was installed on-board the French ATR 42 environmental research aircraft of Safire. The flight height was around 1100 m above the site which led to a Ground Sampling Distance (GSD) of 0.75 m. This image had a spectral resolution ranging from 3.3 in the Visible-Near-InfraRed domain (VNIR, [380–980 nm]) to 7.8 nm in the Short-Wave InfrarRed domain (SWIR, [980–2500 nm]). After radiometric corrections taking into account the instrument calibration and the silica plane window transmission, atmospheric corrections using COCHISE (atmospheric COrrection Code for Hyperspectral Images of remote-sensing SEnsors) were applied (Miesch et al., 2005). The image was then projected on a geographic grid. Finally, the image obtained represented the top-of-canopy spectral reflectance with a spatial resolution of 0.75 m in the [380–2500 nm] domain. Because of the low signal-to-noise ratio (SNR), bands with atmospheric transmission below 80% were excluded, as described in Erudel et al. (2017). A Savitzky-Golay spectral smoothing filter was also applied, with a window size of 5 and a polynomial degree of 2 for both *in-situ* and airborne data. Due to the flight line footprint, five of the control pines were not covered by the hyperspectral image. 15 Aleppo and 15 Stone pines in the contaminated and control sites were then captured. Crowns were delineated manually, avoiding shadowed pixels, and covered 1 to 74 pixels (median of 7 pixels by crown, mean of 10 pixels). Fig. 4 represents the extracted hyperspectral images of the contaminated and control areas with the delineated tree crowns. All pixels of each crown were spatially averaged to retrieve each pine spectral signature. Fig. 5 shows a subset of *in-situ* (considered as needle scale) and airborne (mentioned as canopy scale) spectral signatures for the same trees, according to soil PTE exposure.

Table 1
Structural traits measured in situ. DBH: Diameter at Breast Height.

Traits	Level	Number of replicates
Height	Tree	–
DBH	Tree	–
Length	Needle	5
Width	Needle	5

2.5. Method

The method was based on a linear bivariate regression analysis between different sets of variables built with laboratory, *in-situ* and airborne measurements. Vegetation traits (pigments, structural and biophysical parameters) were then linked to soil PTEs to select the most sensitive parameter for each soil PTE (§ 2.5.1). Secondly, the measured or transformed spectral measurements (needle and canopy scales) (§ 2.5.2) and derived vegetation indices (§ 2.5.3) were correlated with selected vegetation parameters and soil PTE contents to provide the most relevant spectral bands to predict soil PTE contents (§ 2.5.4). The specified vegetation indices were compared with vegetation indices

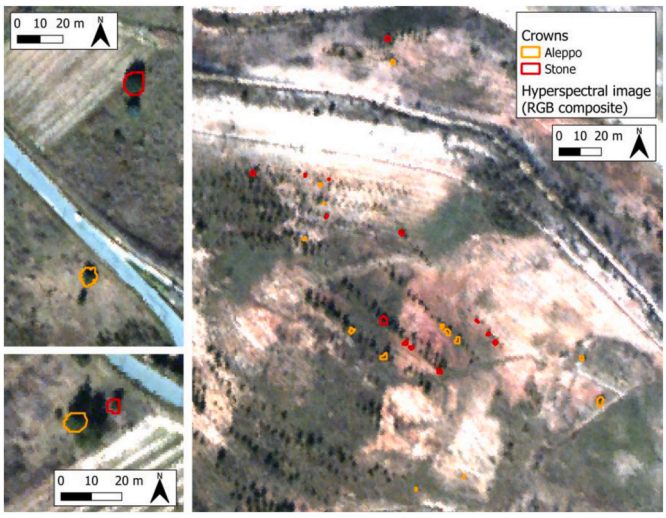

Fig. 4. Extracted images of the hyperspectral flight line and the pine crown delineation. The two left panels show control areas, and the right one the contaminated area.

defined in the literature. This methodology was applied to each species.

2.5.1. Parameter selection

Vegetation traits capturing soil PTE contamination were selected from correlation analysis: the relationship between two variables was assessed with a bivariate linear regression and the Pearson correlation coefficient (r). This correlation analysis has also been led on the components obtained by the dimension reduction technique Principal Component Analysis (PCA) applied to soil PTEs and to pigment concentrations, without conclusive results.

At the end of this stage, for each PTE, at least one sensitive vegetation parameter was retained.

2.5.2. Spectral transformations

Many transformations (normalizations, Continuum Removal-CR, derivatives) were used to process spectral signatures enhancing absorption features in order to retrieve vegetation traits and enhance prediction performance (Erudel et al., 2017; Lassalle et al., 2019b).

2.5.3. Vegetation indices

Two kinds of vegetation indices were retained. Numerous vegetation indices from the literature were applied, mostly designed for pigment retrieval, vegetation health and stress, as well as specific to PTE retrieval; leading to a total of 179 indices covering the reflective spectral domain (Bandaru et al., 2016; Erudel et al., 2017; Fabre et al., 2020; Gimenez et al., 2022; Kupková et al., 2011). The notations and formulas used in these articles were retained for the rest of this study. Only the most suitable indices for our study context are provided in this paper.

New vegetation indices optimized to our context (defined by the species and vegetation traits or PTEs studied) were specified. The index formula retained was:

$$VI(A,B) = \frac{(\rho_B - \rho_A)}{(\rho_B + \rho_A)} \quad (1)$$

with ρ_A the reflectance of the spectral band A in nm, and same for B.

The next step of the methodology relied on assessing the correlation between all possible two-band combinations in equation (1) and vegetation parameters like pigment concentrations and/or each of the nine metal contents. Correlation maps of the square Pearson correlation

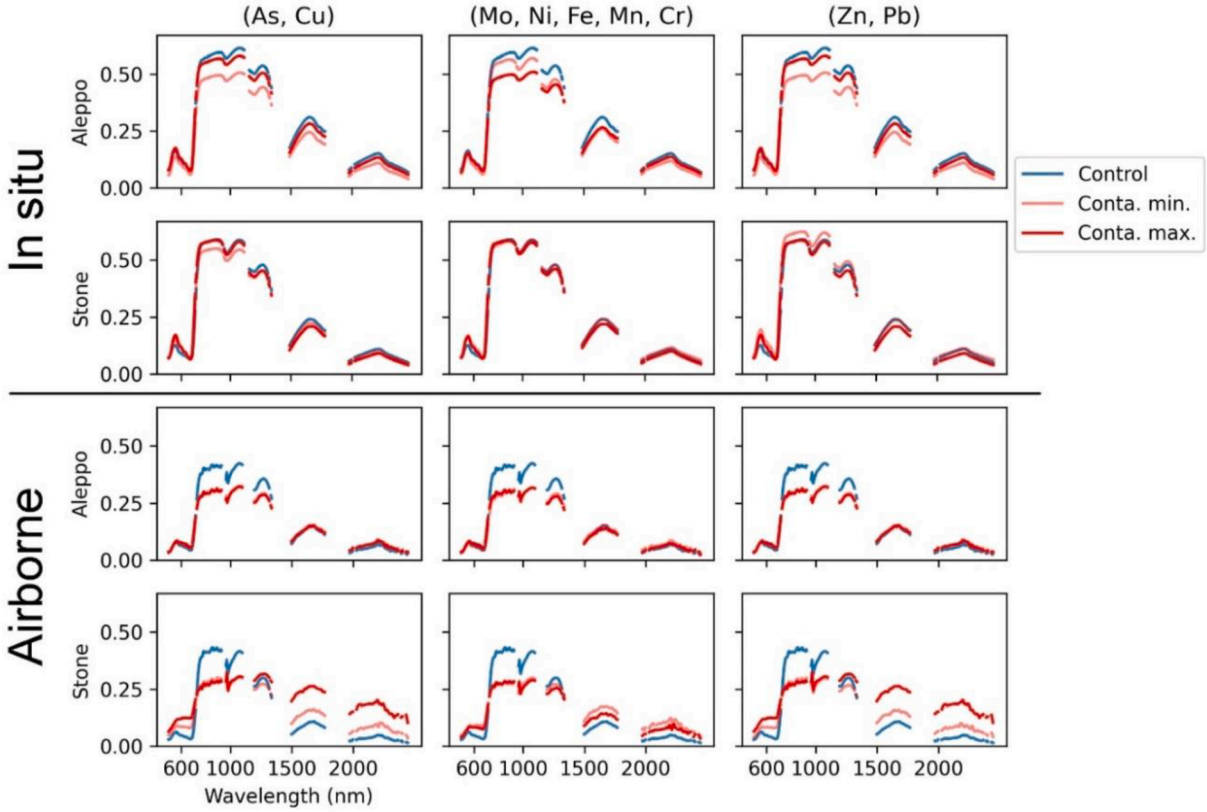

Fig. 5. At needle and canopy scales and for both species, spectral signatures of the pines in the control and contaminated (Conta.) areas. Based on the groups resulting from the Pearson correlation coefficient values between PTEs (Fig. 3b), for each PTE group, the pines with the minimum (min.) and maximum (max.) PTE exposures were retained. This exposure per pine was calculated as the median of normalized PTE soil contents in the group.

coefficient were produced and thresholded in order to keep the optimized spectral band pairs for both needle and canopy scales (§ 2.3.3, § 2.4).

To summarize, two kinds of spectral indices were defined and selected:

The indirect spectral indices specific to a vegetation parameter sensitive to PTEs in soil:

- VI-<variable> (A,B): spectral index suited, regardless the species, for a given sensitive vegetation parameter <variable> like chlorophyll concentration (with A and B the spectral bands in the index formulation (1)),
- VI-<species><variable>(A,B): index specified for a given <species> (defined by Al for the Aleppo and St for the Stone pine species), and sensitive to the vegetation parameter defined by <variable>,

The direct spectral indices sensitive to PTEs in soil: noticed VI-(A,B) regardless the species and VI-<species>(A,B) for the given <species> (Al for Aleppo or St for Stone pine species).

2.5.4. Spectral correlation analysis

The correlation analysis between spectral values (i.e. spectral signatures, transformed signatures or vegetation indices) and vegetation parameters was performed according to the methodology described in section 2.5.1. The same correlation analysis concerning these spectral values and soil PTEs was led.

3. Results

3.1. Relation between vegetation parameters and soil PTE contents

Looking at the measured pigments of the Aleppo pine needles, the carotenoid and chlorophyll concentrations were linked with significant (p-value <0.05) results to 4 soil PTEs: Cu, Ni, Fe Mn, plus Mo for chlorophylls (absolute r varied between 0.54 and 0.75; Table 2). The best results occurred for Cu (r of −0.73 and −0.75 for carotenoids and chlorophylls, respectively). The correlation values were similar for the two pigment families. For the Stone pines, pigments seemed less correlated with soil PTEs than for the Aleppo pines: the r values (significant results) were higher than 0.5 only for As (r of −0.52 and −0.58 for chlorophylls and carotenoids, respectively) and Ni with carotenoids (r = −0.52). The pigments of Stone pine samples provided better significant correlations to As in soil than the one of the Aleppo pines.

The needle water contents had no significant correlation with PTE contents (Table 3). For the Aleppo pines, the highest coefficients of correlation were for Ni and Cr (r of 0.53 and 0.68 respectively). For Stone pine needle, PTEs the highest r value was 0.53 for Zn.

No measured structural trait of the Aleppo pines at needle or canopy scaleswas significantly correlated with any soil PTE in our context (Table 4). For the Stone pine, the best result was obtained for Zn with the needle length (r = 0.73, p-value <0.01). The mean difference of needle lengths between the Stone pines of the contaminated and reference sites was around 1 cm, but not significant at a 0.05 level (mean length of 9.1 cm and 10.1 cm respectively). For this species, significant (with p-value <0.05) correlation values higher than 0.55 were also observed for the needle length and DBH with Pb and needle width with Cu.

3.2. Exploitation of the needle spectral signatures

The spectral signatures of needle samples were used to assess pigment contents. Among the spectral indices tested for Aleppo pine, NDLI (Normalized Difference Lignin Index) performed the best (r = 0.88 for chlorophylls, r = 0.87 for carotenoids, significant results with p-value <0.01). NDLI is using the 1680 nm and 1754 nm bands, two bands mainly sensitive to lignin (Fourty et al., 1996; Serrano et al., 2002). Other indices presented also high correlations (over 0.85). Two new spectral indices VI-AlChl(593, 1203) and VI_Chl(610, 1687) provided similar significant (p-value <0.01) performance with r values of 0.87. MCARI (Modified Chlorophyll Absorption Ratio Index), sensitive to anthocyanin and chlorophylls and combining spectral bands (550, 705 and 750 nm), and IRECI (Inverted Red-Edge Chlorophyll Index), which incorporates the reflectance in four spectral bands (665, 705, 740 and 783 nm) to estimate canopy chlorophyll contents, were selected to be sensitive to carotenoids in our context (r values between 0.86 and 0.87, significant results with p-value <0.01) (Daughtry et al., 2000; Frampton et al., 2013).

The r values of Stone pine species were higher than those of Aleppo pine species. Curvature Index (CI) performed the best considering the chlorophyll contents (|r| = 0.95, p-value <0.01). This index related to chlorophyll fluorescence is a function of the reflectance values at the 675, 690 (originally 691 and 683 nm) spectral bands (Zarco-Tejada et al., 2000). The specified indices, VI_StChl(597, 1656), VI_StChl(610, 1630) and VI_Chl(610, 1687), provided similar performance for chlorophyll prediction with r values of 0.94 (p-value <0.01). The best assessments of Stone pine species for carotenoid contents were obtained with the specified indices, VI_StChl(610, 1630) and VI_StChl(597, 1656) (r values equal to 0.94, p-value <0.01). The indices sensitive for both chlorophylls and carotenoids, CI and VI_StChl(610, 1630), provided similar performance.

For the Stone pine, the NDLI index which performed well for Aleppo pine had an r value of 0.68 and 0.80 for chlorophylls and carotenoids (p-values <0.01), respectively. For the Aleppo pine, CI, considered as the best-performing for the Stone pine, had an absolute r value of 0.50 and 0.39 (not significant).

According to the relation between chlorophylls/carotenoids and soil PTE contents (§ 3.1), and the significant correlation between NDLI and CI and these pigments, PTE contents were assessed with pigment predictions. For Aleppo pine species, Cu, Ni, Cr and Fe were predicted with r values higher than 0.7 (p-value <0.01, except for Cr < 0.05). Mn and Mo had less satisfactory significant performance, and pigments could not predict As, Zn and Pb contents at significant levels (Table 5). The results showed no difference between chlorophyll and carotenoid intermediate estimation. The poor scores for Stone pines showed no significant relationship between needle pigments and soil PTEs (Table 2).

The existing vegetation indices and the new spectral indices were also used to directly assess the soil PTE contents. The best result for each pine species and metal element is provided in Table 6. Fig. 6 represents for the Aleppo pine the predicted soil PTE contents according to the measured contents for each PTE. Higher scores were obtained with direct spectral indices (Table 6) in comparison to the indirect assessment by the mean of pigment concentration prediction (Table 5). The most

Table 2
Pearson r coefficient values for pigment – soil PTE parameters. Car.: carotenoids, Chl.: total chlorophyll (a+b). Bold values indicate |r| > 0.50.

Species	Pigment	Cu	As	Ni	Cr	Fe	Mn	Mo	Zn	Pb	No. of samples
Aleppo	Chl.	**-0.75**†	-0.50	**-0.70***	**-0.62**	**-0.62***	**-0.61***	**-0.57***	0.05	0.35	8–13
	Car.	**-0.73**†	-0.49	**-0.67***	**-0.63**	**-0.59***	**-0.58***	**-0.54**	0.05	0.38	12–15
Stone	Chl.	0.06	**-0.52***	-0.38	0.05	-0.22	-0.23	-0.18	0.28	0.35	8–13
	Car.	-0.06	**-0.58***	**-0.52***	-0.07	-0.41	-0.38	-0.36	0.30	0.38	12–15

*value significant at a level of 0.05; † value significant at a level of 0.01. The number of samples is provided in the last column.

Table 3
Pearson r coefficient values for needle Water Content (WC) – soil PTE. Bold values indicate |r| > 0.50. No value was significant at a level of 0.05. The number of samples is provided in the last column.

Species	Cu	As	Ni	Cr	Fe	Mn	Mo	Zn	Pb	No. of samples
Aleppo	-0.42	-0.28	**-0.53**	**-0.68**	-0.48	-0.42	-0.42	0.35	0.48	8–13
Stone	0.07	-0.15	-0.32	0.10	-0.31	-0.17	-0.21	**0.53**	0.50	12–15

Table 4
Pearson r coefficient values for structural traits – soil PTE. Each trait was defined by its measurement scale: T for Tree and N for Needle. Bold values indicate |r| > 0.50.

Species	Parameter	Cu	As	Ni	Cr	Fe	Mn	Mo	Zn	Pb	Nb. of samples
Aleppo	T-Height	-0.39	-0.47	-0.18	-0.05	-0.24	-0.26	-0.21	-0.09	-0.09	11–17
	T-DBH	-0.30	-0.42	-0.38	-0.27	-0.31	-0.28	-0.30	0.13	0.09	12–18
	N-Length	-0.37	-0.50	-0.31	-0.23	-0.28	-0.39	-0.24	0.50	0.11	8–13
	N-Diameter	-0.18	-0.22	-0.09	0.12	-0.11	-0.16	-0.11	0.24	0.04	8–13
Stone	T-Height	-0.34	-0.40	-0.43	0.21	-0.24	-0.33	-0.12	-0.06	-0.03	12–15
	T-DBH	0.29	-0.38	-0.33	0.06	-0.30	-0.29	-0.43	0.26	**0.55***	14–17
	N-Length	0.18	-0.10	-0.20	0.09	-0.15	-0.12	-0.29	**0.73**†	**0.62***	12–15
	N-Diameter	**0.54***	-0.11	0.29	0.42	0.41	0.25	0.08	0.38	0.34	12–15

To conclude, Stone pines seemed less sensitive than Aleppo pines to soil PTEs. Stone pines had a different behaviour when confronted to soil contamination and it seemed that the needle length was the most impacted structural parameter. Pigment concentrations were the most promising parameters to predict soil PTEs. They have been then retained in the next to estimate soil PTE contents.
*value significant at a level of 0.05; † value significant at a level of 0.01. The number of samples is provided in the last column.

Table 5
Pearson r coefficient values between predicted and measured soil PTEs, indirectly estimated at the needle scale from pigment prediction. The values are similar between chlorophylls and carotenoids. Bold values are for |r| > 0.50.

Pine species	Cu	As	Ni	Cr	Fe	Mn	Mo	Zn	Pb
Aleppo (NDLI)	**0.70**†	0.42	**0.77**†	**0.78***	**0.70**†	**0.66***	**0.66***	0.11	0.28
Stone (CI)	0.04	0.42	0.44	0.07	0.25	0.25	0.16	0.28	0.29

* value significant at a level of 0.05; † value significant at a level of 0.01.

Table 6
Pearson r coefficient values for soil PTE prediction with spectral indices applied to *i*needle spectral measurements.

Pine species	Cu	As	Ni	Cr	Fe	Mn	Mo	Zn	Pb
Aleppo	-0.89†	-0.73†	0.84†	0.92†	0.80†	0.78†	0.85†	-0.52	-0.56*
Index	VI-*Al* (525,1216)	VI-*Al*(504,1687)	PSRI	VI-*Al*(682,1222)	PSRI	REP_LI VI_Al(693, 1203)	PSRI	CACOI	PSRI
Stone	0.52*	-0.61*	0.76†	0.64*	0.81†	0.78†	0.73†	0.65*	0.50
Index	SWIR_a_WP	MSAVI	SWIR_a_WP	VI-(772,879)	SWIR_a_WP	SWIR_a_WP	SWIR_a_WP	GITELSON	DATT3

* value significant at a level of 0.05; † value significant at a level of 0.01.

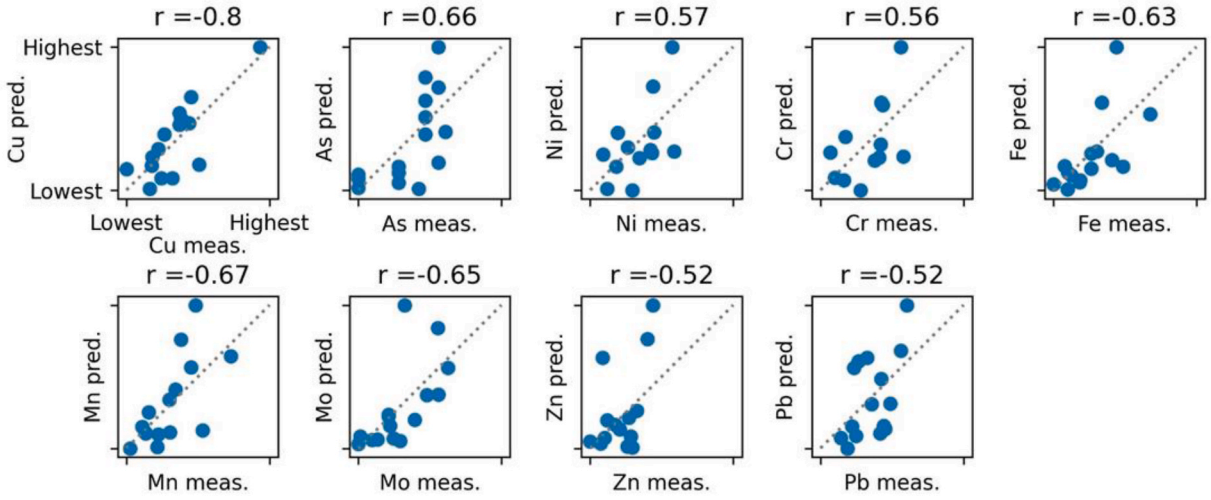

Fig. 6. Measured and predicted PTE soil contents for the Aleppo pines with selected indices applied to needle spectral reflectances (Table 6). pred.: predicted, meas.: measured.

significant results occurred for the Aleppo pine. Most of the good-matching indices were obtained with our newly developed indices (e.g. for Cu, As, Cr). For the Aleppo pine species, 7 PTEs (Cu, As, Ni, Cr, Fe, Mn and Mo) were predicted with r between 0.73 and 0.92 (p-values <0.01). Only Zn and Pb were assessed with a lower performance. The specified indices were selected for Cu, As and Cr: VI-Al (525, 1216), VI-Al(504, 1687) and VI-Al(682, 1222) respectively. The assessment of As, Cu and Cr contents needed new specific-context indices as no index in the literature reached this performance. For other PTEs, existing indices provided the best results. PSRI (Plant Senescence Reflectance Index) using 500, 678 and 750 nm spectral bands was retained for the predictions of Ni, Fe, Mo and Pb contents (Merzlyak et al., 1999). The Red-Edge Position Linear Interpolation (REP_LI) based on spectral bands 700, 740, 780, 800 nm sensitive to chlorophyll provided the best assessment of Mn contents (Guyot and Baret, 1988). CACOI (CArotenoid COncentration Index) (using spectral bands at 515 and 550 nm) was selected for Zn (Gitelson et al., 2003). For Mn, a result identical to the one obtained with the literature indices was achieved using VI_Al(693, 1203). The Stone pine was more sensitive to Ni, Fe, Mn and Mo than to the other PTEs with r values higher than 0.73 (p-values <0.01). Higher performance was reached for Zn in comparison to the one obtained with Aleppo pines. Like for Aleppo pine species, the estimation of the Pb contents with the needle spectral signatures seemed compromised. Among the selected indices, only one new context-specific index VI-(772, 879) was retained for Cr. Cu, Ni, Mn, Fe and Mo were predicted with SWIR_a_WP, corresponding to the spectral position of the maximum first derivative on the interval [1410–1810 nm] correlated to the water contents of the canopy (Erudel et al., 2017). Finally, three sensitive chlorophyll indices, MSAVI (Modified Soil Adjusted Vegetation Index) (Qi et al., 1994), the reflectance ratio at wavelength 700 nm (Gitelson et al., 1999) and DATT3 using 550, 708, 860 nm spectral bands (Datt, 1998) were exploited to predict As, Zn and Pb, respectively.

3.3. Exploitation of the airborne image

The exploitation of *in-situ* spectral response at needle sample scale (§ 3.2) exhibited that the pigment assessment to estimate soil PTE contents in an indirect way (Table 5) had a lower score and lesser significance than direct soil PTE indices (Table 6). The direct estimation was retained to process the airborne image using the existing and context-specific spectral indices.

The best performing index for each soil PTE content prediction is provided in Table 7. Fig. 7 shows an example of the Pearson r maps at both scales used to define the new context-specific index for prediction of Cu contents in soil. For the Aleppo pine species, the maximum correlation was obtained for spectral bands at 518 and 1216 nm at needle scale and 1674 and 1681 nm at canopy scale. The correlation maps of the other PTEs are provided in Fig. S2.

Values for the r coefficient were lower (not significant for four values) than those obtained with the needle spectral signatures (r range, for Aleppo pines, between 0.52 and 0.80 at the canopy scale and between 0.56 and 0.92 at the needle scale). For Aleppo pines, the highest deviation according to scale change was obtained for Cr (deviation of 39% between the needle and canopy scales) and the lowest deviation was obtained for Cu and As (deviation of 9–10%), not mentioning Zn and Pb which led to the worst results. For the Stone pine, the highest deviation was related to Cr and Pb. It was not possible to significantly predict Cr using Stone pine spectral response at the canopy scale. In addition, better assessments were made for Pb at canopy scale (p-values <0.05). The lowest deviations between needle and canopy scales were obtained for As, Mn and Zn (deviations bellow 12%). There were only two indices used at both scales but not in the same context (PTE, species): SWIR_a_WP and VI-Al(597, 1656) (the same as VI_StChl(597, 1656)).

The sensitivity to soil PTEs according to species was particularly less significant at canopy scale than at needle level. At canopy scale, better performance was obtained for As, Ni, Mn, Zn and Pb predictions considering Stone pines. This difference was the most important for Zn and Pb (deviation of 17% and 28% for Zn and Pb between the Aleppo and Stone pine species, respectively). As, Ni, Mn and Mo led to the lowest deviations between species (below 5%).

For Aleppo pine, five soil PTEs (Cu, As, Fe, Mn, Mo) were assessed with r values higher than 0.63 (p-values >0.01). The best performances were for Cu prediction and equivalent results were obtained with a context-specific index and NDNI (Normalized Difference Nitrogen Index) using spectral bands at 1510 and 1680 nm (Serrano et al., 2002). Mn and Fe were assessed with the same new index VI-Al(597,1656). This index is the same as VI_StChl(597, 1656) used to predict the carotenoid contents of Stone pine. VI-(772, 879) was selected to estimate Ni and Cr (not significant for Cr). For As, Mn, Zn (not significant) and Pb, the following existing indices were retained respectively: SWIR_a_WP, NDNI and CAI (Cellulose Absorption Index based on the 2000, 2100 and 2200 nm spectral bands) (Nagler et al., 2000).

For Stone pine, five soil PTEs (As, Mn, Mo, Zn and Pb) were predicted with r values equal to or above 0.63 (p-values <0.05). The highest performance was obtained for Pb with the Modified Anthocyanin Reflectance Index (MARI) using spectral bands at 550, 700, 800 nm (Gitelson et al., 2001, 2009). This index was also retained to assess Zn. The new index VI-St(497,1518) was selected for Fe, Mn and Mo predictions. As was assessed with VI-St(518,2341). The Photochemical Reflectance Index (PRI) (using spectral bands at 531, 570 nm) used in literature for stress detection was selected for Ni (Gamon et al., 1992).

The indices selected in Table 7 at canopy scale had poor performance at needle scale. Only three of them had an r-value higher than 0.50 at needlescale for Aleppo pine: VI-Al(504, 1687) for Cu, VI-Al(597, 1656) for Fe and VI-Al(597, 1656) for Mn.

Some indices had however higher or similar (significant) prediction abilities for the Aleppo pines considering both needle and canopy scales (Table 8). No index was adapted to both scales for the Stone pines.

4. Discussion

4.1. Link between soil PTE contents and vegetation traits

Many studies mentions that PTE stress could produce some changes in plant morphological and biochemical characteristics and some of them suggests that heavy metal stress reduced pigment contents for various species (Lassalle et al., 2021; Mirzaei et al., 2019; Li et al., 2015; Shin et al., 2019). This point is confirmed by our results in particular for Aleppo pine: the most relevant vegetation traits among those measured

Table 7
Pearson r coefficient values for soil PTE prediction with spectral indices at canopy scale.

Pine species	Cu	As	Ni	Cr	Fe	Mn	Mo	Zn	Pb
Aleppo	-0.80†	0.66†	0.57*	0.56	-0.63*	-0.67†	-0.65†	-0.52	-0.52*
Index	VI-*Al*(504,1687) NDNI	SWIR_a_WP	VI-(772,879)	VI-(772,879)	VI- *Al*(597,1656)	VI- *Al*(597,1656)	NDNI	CAI	CAI
Stone	-0.42	-0.68†	-0.59*	0.28	-0.51	-0.71†	-0.63*	-0.63*	-0.73†
Index	VI-(772,879)	VI-*St*(518,2341)	PRI	SWIR_a_WP	VI-*St*(497,1518)	VI-*St*(497,1518)	VI-*St*(497,1518)	MARI	MARI

* value significant at a level of 0.05; † value significant at a level of 0.01.

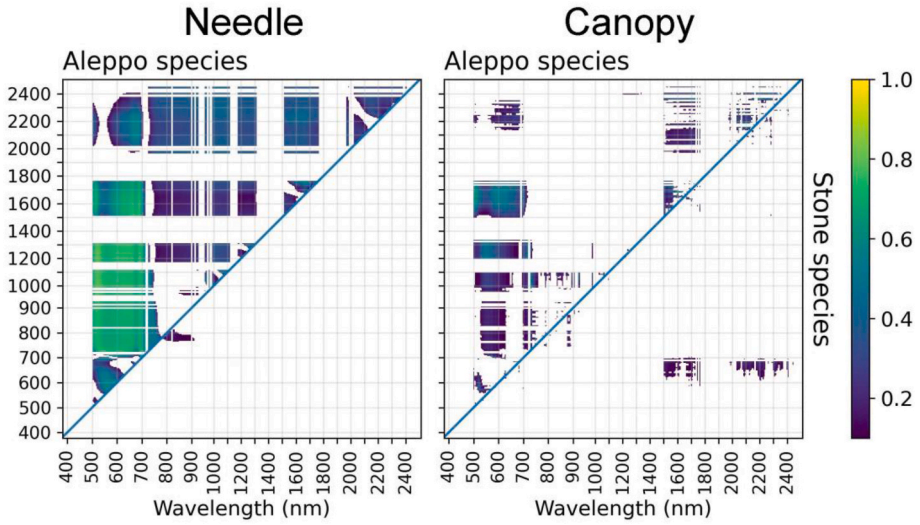

Fig. 7. Correlation maps of Pearson r scores for the definition of a new optimized index relative to Cu soil contents, at needle and canopy scales. Each correlation map is divided in two parts: upper-left corner for Aleppo pine and bottom-right for Stone pine.

Table 8
Pearson r coefficient values at both needle and canopy scales, and the mean of their absolute values, for soil PTE prediction with spectral indices for Aleppo pines. Only mean r of 0.60 or more are represented.

PTE	Index	Mean absolute r	Needle r	Canopy r
Cu	VI-*Al*(504,1687)	0.79	0.79†	0.80†
Ni	VI-*Al*(710,1203)	0.62	0.71†	0.52
Fe	VI-*Al*(710,1203)	0.63	0.66*	0.60*
Mn	VI-*Al*(555,1203)	0.68	0.76†	0.60*

* value significant at a level of 0.05; † value significant at a level of 0.01.

to characterize soil contaminations were the chlorophyll and carotenoid pigments for this species. Several metal elements are essential for optimum plant growth and development. They however become phytotoxic from a certain level depending on various factors such as the species and its growth and phenological stages, the soil characteristics and the type of metal and its speciation. It is difficult to propose a threshold for the toxic concentration of each metal (Datt, 1998; Lassalle et al., 2021).

Previous studies observe dramatic reductions in chlorophyll contents with As accumulation in rice plants (Bandaru et al., 2016). These changes are attributed to damages of the leaf chloroplast membrane structures associated with As toxicity (Rahman et al., 2007). In our study, the correlation between As metalloid and measured pigments of Aleppo pine samples was not established, at the opposite of other metals like Cu, Ni, Fe, Mn.

Even if Pb strongly inhibits plant growth, chlorophyll production, and water contents, no significant correlation was observed between measured pine traits and Pb contents in soil except needle length and trunk diameter. A similar conclusion was drawn for Zn, only significantly correlated to needle length. The behavior of PTEs in soil like Pb, and its impact on plants, is controlled by many factors that could explain the limited correlation with measured vegetation parameters: its bioavailable concentration, its speciation but also the soil pH, the soil particle size, the cation-exchange capacity, the root surface area and/or even the root exudation (Pourrut et al., 2011). Some studies also mention that contaminant effects should be determined not only by the total content of PTEs but also by their potential synergistic interactions, even at low individual concentrations (Pietrzykowski et al., 2014).

In our context, two pine species have been simultaneously planted for phytostabilisation purpose and some control pines are of similar age. Even if significant height differences were observed between the contaminated and the control areas, tree height was not significantly correlated to contamination level. Structural behaviour differences were observed between Aleppo and Stone pines. The needle length of Stone pines seemed to be correlated to two metals (Zn, Pb). The structural trait analysis in relation to PTE contamination is an under-researched topic. Kozlov et al. evaluate the needle fluctuating asymmetry response to environmental pollution nearby a nickel-copper smelter and identify a difference in needle lengths of Scots pines (Kozlov and Niemela, 1999). A recent study on five pine species suggests that needle size strongly influences their anatomy, which, in turn, impacts the mechanical traits and physiological capacities (Wang et al., 2018). The difference in needle length among Stone pines could be considered as a proxy to detect soil contamination in the future. Further investigations are necessary to define if other structural parameters at tree scale like crown size, branch scale (diameter, length) or related to the characteristics of needle foliage (e.g. projected area or total surface area) are sensitive to soil PTEs.

4.2. *Assessment of pigment contents: new indices vs literature indices*

Leaf biochemical and structural parameters were rarely measured simultaneously with spectral measurements (Rautiainen et al., 2018). SWIR wavelengths data are often missing in contamination studies. Our study addressed these two limitations of the literature.

Most of the published work is based on the inversion of leaf radiative transfer models such as PROSPECT or LIBERTY (Leaf Incorporating Biochemistry Exhibiting Reflectance and Transmittance Yields) to retrieve pigment contents in pine needles (Dawson et al., 1998; Jacquemoud and Baret, 1990; Moorthy et al., 2008; Lin et al., 2018; Zarco-Tejada et al., 2004). Some other studies are based on empirical algorithms using one or a few spectral indices in order to prove the correlation between spectral response and pigments concentrations in needles of pine species (Gamon and Berry, 2012; Kovãc et al., 2012; Kupková et al., 2011). The studied species are not Stone and Aleppo pines.

In our study, many published indices for a wide range of species and new context-specific indices were compared to assess chlorophylls and carotenoids concentrations in needles of both Aleppo and Stone pine species.

For these species, most of the powerful specific-context indices use a spectral band in the spectral region sensitive to photosynthetic pigments (e.g. 510, 597, 610 or 693 nm) and another one in the SWIR spectral domain (e.g. 1203, 1630, 1656 or 1687 nm) showing absorption features of water contents in foliage and other chemicals (cellulose, lignin,

nitrogen …) (Gitelson and Merzlyak, 1998).

The spectral response of Stone pines was more sensitive to pigment content variations than the one of Aleppo pines. Some indices in the literature have similar performance to these new indices. VI_StChl (610,1630) was selected for the Stone pine, providing similar performance for chlorophyll and carotenoid predictions. CI, well-known to be sensitive to slight variations in the chlorophyll contents for various types of plant, was well-adapted to assess pigment contents in complement to the new indices for Stone pine.

For Aleppo pine, NDLI, suited to determine biochemical concentrations (nitrogen and lignin) and canopy structural features for a wide range of species, provided a high significant correlation with pigment contents and had a higher sensitivity in comparison to indices referring to photosynthetic pigments like MCARI or IRECI (Curran, 1989). A recent study in the frame of the agricultural field led by Bloem and al. shows a very high correlation of NDLI with dry matter and a high correlation with chlorophyll and carotenoid contents (Bloem et al., 2020).

4.3. Prediction of soil PTE contents: direct and indirect approach comparison

At needle sample scale, existing or context-specific vegetation indices were defined to directly predict soil PTE contents, as well as through the intermediate prediction of a sensitive vegetation parameter, being the pigment contents (chlorophylls and carotenoids). The relationship between soil PTE contents and needle pigment contents s was more significant and stronger for Aleppo pine, and it was similar for the two pigment families. Although some metals or metalloids were indirectly significantly correlated to vegetation indices, there was a significant (p-value <0.05) difference with direct estimations. There was a mean loss of absolute Pearson's r of 0.2 and 0.4 from direct to indirect estimation for the Aleppo and the Stone pines, respectively. Considering the high ability to predict pigments with vegetation indices ($r > 0.87$, p-values <0.01), the correlation loss reasonably comes from the lower and only partially significant pigment – soil PTE relationship (Table 2).

Many studies observe a photosynthetic pigment, chlorophyll-a and -b, concentration loss with increasing PTE exposition for various plant species, especially for rice and soil As (Azizur Rahman et al., 2007; Bakshi et al., 2018; Caporale et al., 2013; Shakya et al., 2008). Shi et al. developed a three-band vegetation index sensitive to total chlorophyll of rice - (Oryza sativa L.) for the direct estimation of soil As contents (significant absolute r of 0.67) (Shi et al., 2016). For Aleppo pine, we obtained good predictions of Cu, Ni, Cr, Fe contents in soil through NDLI, retained for pigment estimation (r values higher than 0.70, p-values <0.05). Non significant correlation scores were obtained for most of the elements with Stone pine. The foliar pigment vs. soil PTE content correlation score was specific to the metal or metalloid and the species.

Some studies are based on the correlation between the pigment and the foliar PTE contents related to the soil underneath. Shin et al. observe that the As contents of the pine needles (*Pinus densiflora*) and the soil underneath are highly correlated, indicator of a transfer of As from soil to pine needles (Shin et al., 2019). They propose a regression model to predict needle As contents by the spectral variation of pine needles. In our study, the r values of As predictions for Aleppo and Stone pines were lower than those obtained for some other metals. These pine species may be less sensitive to As than to other metals like Ni, Cu, Fe, Mn and Mo. To complete our analysis, needle samples have been conserved to measure PTE contents in needles in the future. The direct approach, based on the correlation between needle spectral variation and each metal or metalloid content in soil, is the most promising for the two species at needle and canopy scales. This kind of approach has been little investigated as most published studies are based on leaf metal content assessment (Bandaru et al., 2016; Mirzaei et al., 2019; Shin et al., 2019). Pb and Zn contents are the most difficult to estimate considering both scales and species.

For future works, it will be interesting to assess the performance of multiple linear regression models, especially for specific cases (species, PTE) for which two indices have an equivalent performance such as (Aleppo, Cr) or (Aleppo, Cu).

4.4. Up-scaling management

Performance at needle scale (*in-situ* measurement) was better than at canopy scale (airborne measurement) as mentioned in other studies (Erudel et al., 2017; Lassalle et al., 2019b, 2021). For the Aleppo pine species, r reached a value of 0.92 at needle scale and 0.80 at canopy one.

The choice of the best index for quantifying a given soil PTE depends on the scale of the measurement due to the variation of pine reflectance spectra according to the spatial resolution. At the needle level, the main drivers of reflectance are leaf chlorophyll, water content and inner structure. At canopy scale, additional vegetation traits, like canopy structure (density, shadowing in the crown …) and optical properties of trunks, branches, and understory, systematically decrease canopy reflectance (Rautiainen et al., 2018). In the future, it will be interesting to carry out *in-situ* spectral measurements at canopy scale in order to analyse the robustness of the spectral indices to up-scaling from needle to canopy level.

The part of the studied site composed of reduced crown pines planted in grids can be assimilated to open canopies. In this case, previous studies had difficulties in accurately predicting chlorophyll contents by the red-edge region response due to the direct understory and between-crown shadow impacts (Meggio et al., 2020; Zarco-Tejada et al., 2019). This may explain why the wavelength in the SWIR domain was nearly systematically used in the best-performing indices and in the different indices selected according to needle or canopy level measurements. UAV acquisitions should be investigated to provide an intermediate scale between needle and canopy-level data that could be more suitable to monitor contamination in soil by indirect effects on vegetation (de Castro et al., 2021).

Although the best index selected depended on the spatial resolution, context-specific indices performed well at both scales in order to predict some metal contents in soil using the Aleppo pine species spectral response. The best performance was obtained by VI-Al(504,1687) to estimate Cu at both scales. Some studies have proposed spectral indices to analyse the spectral feature change of Cu stressed leaves for several vegetation types but few have been interested in pine trees and the SWIR bands have not been investigated (Cui et al., 2019; Zhang et al., 2019). Further investigations in other contaminated lands are needed to assess VI-Al(504,1687) robustness to up-scaling for the prediction of soil Cu based on pine spectral reflectance.

4.5. Comparison of species response

It is well known that spectral characteristics associated with PTEs vary between plant species (Slonecker et al., 2010) and, in this regard, according to the species of pine tree (Cindrić et al., 2018). Until now, no study has compared the sensitivity of pine species and studied their specific traits impacted in a contaminated land. Our study addresses this issue.

While the sought relation between soil contamination and pigment contents showed to be statistically significant in the case of Aleppo pine, it was not applicable in the case of Stone pine. A previous study shows that Aleppo pine needles retain high contents of heavy metals in an urban context with long-term soil contamination by Pb, Cd, Cu and Zn (Al-Alawi and Mandiwana, 2007). Unfortunately, no specific information on Stone pine is available. Our study proves that the most sensitive trait of Stone pine to PTE contamination is structural, the length of the needles varying according to the contents of a few PTEs in soil.

In this study, Aleppo pine was the best species for estimating Cu, Fe and Cr contents in soils (not significant at canopy scale for the latter). The best predictions for Zn, Mn and Pb (not significant at needle scale for

the latter) contents in soil were obtained for Stone pine. Equivalent performance was achieved by both species for As, Ni and Mo.

Entry of PTEs from the soil into plants can occur through the roots. Once taken up the PTEs can be immobilized within root tissues or be transported to another plant organ (accumulation of PTEs in their aerial tissues). The transfer of PTEs within the plant, called translocation, can vary considerably depending on the PTE, but also on the tree species.

5. Conclusions

This study aimed to quantify soil PTE contamination in a Sub-mediterranean vegetated area using airborne imagery with very high spatial and spectral resolutions and covering the reflective domain. It focused on nine PTEs and two pine species (Stone and Aleppo) introduced to phytostablize a former ore processing site. A two-step study was proposed according to the observation scale (needle or canopy scales). As a first step, the needle biochemical, biophysical and structural parameters sensitive to soil PTEs were analysed: photosynthetic pigments were the most relevant. The second step compared two approaches (direct and indirect) for each soil PTE content prediction, based on existing or context-specific spectral indices. The direct approach provided the most significant results and was the best performing without the need for additional measurements of pigment contents. The best performing context-specific indices were often based on a spectral band in the SWIR domain, highlighting the importance of this part of the spectrum. Owing to significant uncertainties, Aleppo pine was suitable for Cu, Cr and Fe and Stone pine for Zn, Pb and Mn. Equivalent performances are achieved by both species for As, Ni and Mo. Further investigations will be needed (foliar PTE estimation, PTE bioavailability investigation) to define the pine species to consider as a valuable marker for each PTE in such a context.

We have to acknowledge that the results reported within this study were only based on two pine species from a limited area. This study nonetheless demonstrates the feasibility of the proposed methods for PTE soil content prediction and should be deployed on all pines on the site after automatically identifying the species at tree scale by supervised classification approach based on machine learning algorithms. Promising perspectives of operational use to monitor large contaminated areas will arise in the future with the deployment of hyperspectral UAV sensors and the emergence of new hyperspectral satellite instruments.

Credit author statement

L. Béraud: Methodology, Software, Formal analysis, Investigation, Validation, Writing, Visualization. **Arnaud Elger**: Conceptualization, Methodology, Investigation, Data Curation, Writing, Project administration. **Thomas Rivière**: Software, Investigation, Writing. **Olivier Berseille**: Methodology, Investigation. **Philippe Déliot**: Software, Methodology, Data curation, Writing. **Jérôme Silvestre**: Methodology, Data curation, Writing. **Camille Larue**: Investigation, Writing. **Laurent Poutier**: Software, Methodology, Writing. **Sophie Fabre**: Conceptualization, Methodology, Investigation, Validation, Data Curation, Writing, Visualization, Supervision, Project administration.

Funding

This research was performed in the frame of the APR COMPOST and VITHE projects between ONERA and Lab. Ecologie Fonctionnelle et Environnement, funded by CNES and PNTS (France) respectively.

Declaration of competing interest

The authors declare that they have no known competing financial interests or personal relationships that could have appeared to influence the work reported in this paper.

Data availability

The authors do not have permission to share data.

Acknowledgments

Airborne data was obtained using the aircraft managed by Safire, the French facility for airborne research, an infrastructure of the French National Center for Scientific Research (CNRS), Météo-France and the French National Center for Space Studies (CNES). The authors gratefully acknowledge E. Buffan-Dubau and D. Lambrigot for their assistance in pigment analyses, M. Philippe (CNRS, GEODE) and G. Le Roux (CNRS, LEFE) for p-XRF soil measurements and the site manager.

Appendix A. Supplementary data

Supplementary data to this article can be found online at https://doi.org/10.1016/j.envres.2023.115747.

References

Al-Alawi, M., Mandiwana, K.L., 2007. The use of Aleppo pine needles as a bio-monitor of heavy metals in the atmosphere. J. Hazard Mater. 148 (1–2), 43–46. https://doi.org/10.1016/j.jhazmat.2007.02.001.

Azizur Rahman, M., Hasegawa, H., Mahfuzur Rahman, M., Nazrul Islam, M., Majid Miah, M.A., Tasmen, A., 2007. Effect of arsenic on photosynthesis, growth and yield of five widely cultivated rice (*Oryza sativa L.*) varieties in Bangladesh. Chemosphere 67, 1072–1079. https://doi.org/10.1016/j.chemosphere.2006.11.061.

Bakshi, M., Ghosh, S., Chakraborty, D., Hazra, S., Chaudhuri, P., 2018. Assessment of potentially toxic metal (PTM) pollution in mangrove habitats using biochemical markers: a case study on *Avicennia officinalis L.* in and around Sundarban, India. Mar. Pollut. Bull. 133, 157–172. https://doi.org/10.1016/j.marpolbul.2018.05.030.

Bandaru, V., Daughtry, C.S., Codling, E.E., Hansen, D., White-Hansen, S., Green, C.E., 2016. Evaluating leaf and canopy reflectance of stressed rice plants to monitor arsenic contamination. Int. J. Environ. Res. Publ. Health 13 (6), 606. https://doi.org/10.3390/ijerph13060606.

Barlow, R.G., Cummings, D.G., Gibb, S.W., 1997. Improved resolution of mono- and divinyl chlorophylls a and b and zeaxanthin and lutein in phytoplankton extracts using reverse phase C-8 HPLC. Mar. Ecol. Prog. Ser. 161, 303–307.

Blackburn, G.A., 2007. Hyperspectral remote sensing of plant pigments. J. Exp. Bot. 58 (4), 855–867. https://doi.org/10.1093/jxb/erl123.

Bloem, E., Gerighausen, H., Chen, X., Schnug, E., 2020. The potential of spectral measurements for identifying glyphosate application to agricultural fields. Agronomy 10 (9). https://doi.org/10.3390/agronomy10091409.

Caporale, A.G., Pigna, M., Sommella, A., Dynes, J.J., Cozzolino, V., Violante, A., 2013. Influence of compost on the mobility of arsenic in soil and its uptake by bean plants (*Phaseolus vulgaris L.*) irrigated with arsenite-contaminated water. J. Environ. Manag. 128, 837–843. https://doi.org/10.1016/j.jenvman.2013.06.041.

Cindrić, I.J., Zeiner, M., Starčević, A., Stingeder, G., 2018. Metals in pine needles: characterisation of bio-indicators depending on species. Int. J. Eng. Sci. Technol. https://doi.org/10.1007/s13762-018-2096-x.

Cui, S., Ding, R., Zhou, K., 2019. A new hyperspectral index for estimating copper content in an indicative plant for the exploration of copper deposit. J. Plant Growth Regul. 38, 956–965. https://doi.org/10.1007/s00344-018-9905-9.

Curran, P.J., 1989. Remote sensing of foliar chemistry. Rem. Sens. Environ. 30, 271–278. https://doi.org/10.1016/0034-4257(89)90069-2.

Datt, B., 1998. Remote sensing of chlorophyll a, chlorophyll b, chlorophyll a+b, and total carotenoid content in eucalyptus leaves. Remote Sens. Environ. 66, 111–121.

Daughtry, C., Walthall, C., Kim, M.S., Brown de Colstoun, E., McMurtrey, J.E., 2000. Estimating corn leaf chlorophyll concentration from leaf and canopy reflectance. Rem. Sens. Environ. 74 (2), 229–239. https://doi.org/10.1016/S0034-4257(00)00113-9.

Dawson, T.P., Curran, P.J., Plummer, S.E., 1998. Liberty - modeling the effects of leaf biochemical concentration on reflectance spectra. Rem. Sens. Environ. 65 (1), 50–60.

de Castro, A.I., Shi, Y., Maja, J.M., Peña, J.M., 2021. UAVs for vegetation monitoring: overview and recent scientific contributions. Rem. Sens. 13 (11) https://doi.org/10.3390/rs13112139.

Diepens, N.J., Buffan-Dubau, E., Budzinski, H., Kallerhoff, J., Merlina, G., Silvestre, J., Auby, I., Tapie, Nathalie, Elger, A., 2017. Toxicity effects of an environmental realistic herbicide mixture on the seagrass *zostera noltei*. Environ. Pollut. 222, 393–403. https://doi.org/10.1016/j.envpol.2016.12.021.

Doumas, P., Munoz, M., Banni, M., 2018. Polymetallic pollution from abandoned mines in Mediterranean regions: a multidisciplinary approach to environmental risks. Reg. Environ. Change 18, 677–692. https://doi.org/10.1007/s10113-016-0939-x.

Erudel, T., Fabre, S., Houet, T., Mazier, F., Briottet, X., 2017. Criteria comparison for classifying peatland vegetation types using in situ hyperspectral measurements. Rem. Sens. 9 (7) https://doi.org/10.3390/rs9070748.

Fabre, S., Gimenez, R., Elger, A., Rivière, T., 2020. Unsupervised monitoring vegetation after the closure of an ore processing site with multi-temporal optical remote sensing. Sensors 20 (17), 4800. https://doi.org/10.3390/s20174800.

Feret, J.B., le Maire, G., Jay, S., Berveiller, D., Bendoula, R., Hmimina, G., Cheraiet, A., Oliveira, J.C., Ponzoni, F.J., Solanki, T., de Boissieu, F., Chave, J., Nouvellon, Y., Porcar-Castell, A., Proisy, C., Soudani, K., Gastellu-Etchegorry, J.P., Lefevre-Fonollosa, M.J., 2019. Estimating leaf mass per area and equivalent water thickness based on leaf optical properties: potential and limitations of physical modeling and machine learning. Remote Sens. Environ. https://10.1016/j.rse.2018.11.002.

Fourty, T., Baret, F., Jacquemoud, S., Schmuck, G., Verdebout, J., 1996. Leaf optical properties with explicit description of its biochemical composition: direct and inverse problems. Rem. Sens. Environ. 56 (2), 104–117. https://doi.org/10.1016/0034-4257(95)00234-0.

Frampton, W.J., Dash, J., Watmough, G., Milton, E.J., 2013. Evaluating the capabilities of Sentinel-2 for quantitative estimation of biophysical variables in vegetation. ISPRS J. Photogrammetry Remote Sens. 82, 83–92. https://doi.org/10.1016/j.isprsjprs.2013.04.007.

Gamon, J., Peñuelas, J., Field, C.B., 1992. A narrow-waveband spectral index that tracks diurnal changes in photosynthetic efficiency. Remote Sens. Environ. 41, 35–44.

Gamon, J., Berry, J.A., 2012. Facultative and constitutive pigment effects on the Photochemical Reflectance Index (PRI) in sun and shade conifer needles. Isr. J. Plant Sci. 60 (1).

Gamon, J.A., Somers, B., Malenovský, Z., Middleton, E.M., Rascher, U., Schaepman, M. E., 2019. Assessing vegetation function with imaging spectroscopy. Surv. Geophys. 40, 489–513. https://doi.org/10.1007/s10712-019-09511-5.

Gimenez, R., Lassalle, G., Elger, A., Dubucq, D., Credoz, A., Fabre, S., 2022. Mapping plant species in a former industrial site using airborne hyperspectral and time Series of sentinel-2 data sets. Rem. Sens. 14, 3633. https://doi.org/10.3390/rs14153633.

Gitelson, A.A., Merzlyak, M.N., 1998. Remote sensing of chlorophyll concentration in higher plant leaves. Adv. Space Res. 22, 689–692.

Gitelson, A.A., Buschmann, C., Lichtenthaler, H.K., 1999. The chlorophyll fluorescence ratio F 735/F 700 as an accurate measure of the chlorophyll content in plants. Remote Sens. Environ. 69, 296–302.

Gitelson, A.A., Merzlyak, M.N., Chivkunova, O.B., 2001. Optical properties and nondestructive estimation of anthocyanin content in plant leaves. Photochem. Photobiol. 74, 38–45.

Gitelson, A.A., Gritz, Y., Merzlyak, M.N., 2003. Relationships between leaf chlorophyll content and spectral reflectance and algorithms for non-destructive chlorophyll assessment in higher plant leaves. J. Plant Physiol. 160, 271–282.

Gitelson, A.A., Chivkunova, O.B., Merzlyak, M.N., 2009. Nondestructive estimation of anthocyanins and chlorophylls in anthocyanic leaves. Am. J. Bot. 96, 1861–1868. https://doi.org/10.3732/ajb.0800395.

Guyot, G., Baret, F., 1988. Utilisation de la haute résolution spectrale pour suivre l'état des couverts végétaux. In: Signatures Spectrales d'objets en télédétection. 4 ème Colloque International; Agence Spatiale Européenne: Aussois, France, vol. 287, pp. 279–286.

Homolová, L., Malenovský, Z., Clevers, J., Garcia-Santos, G., Schaepman, M.E., 2013. Review of optical-based remote sensing for plant trait mapping. Ecol. Complex. 15 https://doi.org/10.1016/j.ecocom.2013.06.003.

Jacquemoud, S., Baret, F. PROSPECT, 1990. A model of leaf optical properties spectra, Remote Sensing of Environment. Rem. Sens. Environ. 34 (2), 75–91. https://doi.org/10.1016/0034-4257(90)90100-Z.

Kokaly, R.F., Asner, G.P., Ollinger, S.V., Martin, M.E., Wessman, C.A., 2009. Characterizing canopy biochemistry from imaging spectroscopy and its application to ecosystem studies. Remote Sens. Environ. 113, S78–S91. https://doi.org/10.1016/J.RSE.2008.10.018.

Kovāc, D., Navratil, M., Malenovsky, Z., Stroch, M., Spunda, V., Urban, O., 2012. Reflectance continuum removal spectral index tracking the xanthophyll cycle photoprotective reactions in Norway spruce needles. Funct. Plant Biol. 39, 987–998. https://doi.org/10.1071/FP12107.

Kozlov, M.V., Niemela, P., 1999. Difference in needle length· a new and objective indicator of pollution impact on Scots pine (*Pinus sylvestris*). Water, Air Soil Pollut. 116, 365–370.

Kupková, L., Potůčková, M., Zachová, K., Lhotáková, Z., Kopačková, V., Albrechtová, J., 2011. Chlorophyll determination in silver Birch and Scots Pine foliage from hyperspectral data. In: Proceedings of EARSeL Conference, Zadar, Croatia.

Küpper, H., Andresen, E., 2016. Mechanisms of metal toxicity in plants. Metallomics 8, 269–285. https://doi.org/10.1039/c5mt00244c.

Lassalle, G., Fabre, S., Credoz, A., Hédacq, R., Bertoni, G., Dubucq, D., Elger, A., 2019a. Application of PROSPECT for estimating Total Petroleum Hydrocarbons in contaminated soils from leaf optical properties. J. Hazard Mater. 377, 409–417. https://doi.org/10.1016/j.jhazmat.2019.05.093.

Lassalle, G., Elger, A., Credoz, A., Hédacq, R., Bertoni, G., Dubucq, D., Fabre, S., 2019b. Toward quantifying oil contamination in vegetated areas using very high spatial and spectral resolution imagery. Rem. Sens. 11 (19), 2241. https://doi.org/10.3390/rs11192241.

Lassalle, G., Fabre, S., Credoz, A., Hédacq, R., Dubucq, D., Elger, A., 2021. Mapping leaf metal content over industrial brownfields using airborne hyperspectral imaging and optimized vegetation indices. Sci. Rep. 11 (2) https://doi.org/10.1038/s41598-020-79439-z.

Lausch, A., Erasmi, S., King, D.J., Magdon, P., Heurich, M., 2016. Understanding forest health with remote sensing -Part I—a review of spectral traits, processes and remote-sensing characteristics. Rem. Sens. 8 (1029) https://doi.org/10.3390/rs8121029.

Lemière, B., 2018. A review of pXRF (field portable X-ray fluorescence) applications for applied geochemistry. J. Geochem. Explor. 188, 350–363. https://doi.org/10.1016/j.gexplo.2018.02.006.

Lesaignoux, A., Fabre, S., Briottet, X., 2013. Influence of soil moisture content on spectral reflectance of bare soils in the 0.4–14 μm domain. Int. J. Rem. Sens. 34 (7), 2268–2285. https://doi.org/10.1080/01431161.2012.743693.

Lhotáková, Z., Albrechtová, J., Malenovský, Z., Rock, B.N., Polák, T., Cudlín, P., 2007. Does the azimuth orientation of Norway spruce (*Picea abies/L./Karst.*) branches within sunlit crown part influence the heterogeneity of biochemical, structural and spectral characteristics of needles? EEB 59, 283–292.

Li, X., Liu, X., Liu, M., Wang, C., Xia, X., 2015. A hyperspectral index sensitive to subtle changes in the canopy chlorophyll content under arsenic stress. Int. J. Appl. Earth Obs. Geoinf. 36, 41–53. https://doi.org/10.1016/j.jag.2014.10.017.

Li, D., Tian, L., Wan, Z.F., Jia, M., Yao, X., Tian, Y.C., Zhu, Y., Cao, W.X., Cheng, T., 2019. Assessment of unified models for estimating leaf chlorophyll content across directional-hemispherical reflectance and bidirectional reflectance spectra. Remote Sens. Environ. https://10.1016/j.rse.2019.111240.

Lin, Q., Huang, H., Yu, L., Wang, J., 2018. Detection of shoot beetle stress on yunnan pine forest using a coupled LIBERTY2-INFORM simulation. Rem. Sens. 10, 1133. https://doi.org/10.3390/rs10071133.

Meggio, F., Zarco-Tejada, P.J., Núñez, L.C., Sepulcre-Cantó, G., González, M.R., Martín, P., 2020. Grape quality assessment in vineyards affected by iron deficiency chlorosis using narrow-band physiological remote sensing indices. Remote Sens. Environ. 114, 1968–1986. https://doi.org/10.1016/j.rse.2010.04.004.

Merzlyak, M.N., Gitelson, A.A., Chivkunova, O.B., Rakitin, V.Y., 1999. Non-destructive optical detection of pigment changes during leaf senescence and fruit ripening. Physiol. Plantarum 106, 135–141. https://doi.org/10.1034/j.1399-3054.1999.106119.x.

Miesch, C., Poutier, L., Achard, V., Briottet, X., Lenot, X., Boucher, Y., 2005. Direct and inverse radiative transfer solutions for visible and near-infrared hyperspectral imagery. IEEE Trans. Geosci. Rem. Sens. 43 (7), 1552–1562. https://doi.org/10.1109/TGRS.2005.847793.

Mirzaei, M., Verrelst, J., Marofi, S., Abbasi, M., Azadi, H., 2019. Eco-friendly estimation of heavy metal contents in grapevine foliage using in-field hyperspectral data and multivariate analysis. Rem. Sens. 11 (2731) https://doi.org/10.3390/rs11232731.

Moor, H., Rydin, H., Hylander, K., Nilsson, M.B., Lindborg, R., Norberg, J., 2017. Towards a trait-based ecology of wetland vegetation. J. Ecol. 105, 1623–1635. https://doi.org/10.1111/1365-2745.12734.

Moorthy, I., Miller, J.R., Noland, T.L., 2008. Estimating chlorophyll concentration in conifer needles with hyperspectral data: an assessment at the needle and canopy level. Rem. Sens. Environ. 112 (6), 2824–2838. https://doi.org/10.1016/j.rse.2008.01.013.

Mõttus, M., Hernández- Clemente, R., Perheentupa, V., Markiet, V., 2017. In situ measurement of Scots pine needle PRI. Plant Methods 13 (35). https://doi.org/10.1186/s13007-017-0184-4.

Nagler, P., Daughtry, C., Goward, S., 2000. Plant litter and soil reflectance. Remote Sens. Environ. 71, 207–215.

Ong, C., Carrère, V., Chabrillat, S., Clark, R., Hoefen, T., Kokaly, R., Marion, R., Souza Filho, C.R., Swayze, G., Thompson, D.R., 2019. Imaging spectroscopy for the detection, assessment and monitoring of natural and anthropogenic hazards. Surv. Geophys. 40, 431–470. https://doi.org/10.1007/s10712-019-09523-1.

Parsons, C., Margui Grabulosa, E., Pili, E., Floor, G.H., Roman-Ross, G., Charlet, L., 2013. Quantification of trace arsenic in soils by field-portable X-ray fluorescence spectrometry: considerations for sample preparation and measurement conditions. J. Hazard Mater. 262, 1213–1222. https://doi.org/10.1016/j.jhazmat.2012.07.001.

Peng, Y., Fan, M., Wang, Q., Lan, W., Long, Y., 2018. Best hyperspectral indices for assessing leaf chlorophyll content in a degraded temperate vegetation. Ecol. Evol. 8, 7068–7078. https://doi.org/10.1002/ece3.4229.

Pietrzykowski, M., Socha, J., van Doorn, N.S., 2014. Linking heavy metal bioavailability (Cd, Cu, Zn and Pb) in Scots pine needles to soil properties in reclaimed mine areas. Sci. Total Environ. 470–471, 501–510. https://doi.org/10.1016/j.scitotenv.2013.10.008.

Pourrut, B., Shahid, M., Dumat, C., Winterton, P., Pinelli, E., 2011. Lead uptake, toxicity, and detoxification in plants. Rev. Environ. Contam. Toxicol. 213, 113–136. https://doi.org/10.1007/978-1-4419-9860-6_4.

Qi, J., Chehbouni, A., Huete, A., Kerr, Y., Sorooshian, S., 1994. A modified soil adjusted vegetation index. Remote Sens. Environ. 48, 119–126.

Rahman, M., Hasegawa, H., Rahman, M., Islam, M., Miah, M., Tasmen, A., 2007. Effect of arsenic on photosynthesis, growth and yield of five widely cultivated rice (Oryza sativa L.) varieties in Bangladesh. Chemosphere 67, 1072–1079. https://doi.org/10.1016/j.chemosphere.2006.11.061.

Ran, J., Wang, D., Wang, C., Zhang, G., Yao, L., 2014. Using portable X-ray fluorescence spectrometry and GIS to assess environmental risk and identify sources of trace metals in soils of peri-urban areas in the Yangtze Delta region, China. Environ. Sci.: Process. Impacts 16, 1870–1877. https://doi.org/10.1039/c4em00172a.

Rautiainen, M., Lukeš, P., Homolová, L., Hovi, A., Pisek, J., Mõttus, M., 2018. Spectral properties of coniferous forests: a review of in situ and laboratory measurements. Rem. Sens. 10, 207. https://doi.org/10.3390/rs10020207.

Serrano, L., Peñuelas, J., Ustin, S.L., 2002. Remote sensing of nitrogen and lignin in Mediterranean vegetation from AVIRIS data: decomposing biochemical from structural signals. Rem. Sens. Environ. 81, 355–364. https://doi.org/10.1016/S0034-4257(02)00011-1.

Shakya, K., Chettri, M.K., Sawidis, T., 2008. Impact of heavy metals (copper, zinc, and lead) on the chlorophyll content of some mosses. Arch. Environ. Contam. Toxicol. 54, 412–421. https://doi.org/10.1007/s00244-007-9060-y.

Shi, T., Liu, H., Chen, Y., Wang, J., Wu, G., 2016. Estimation of arsenic in agricultural soils using hyperspectral vegetation indices of rice. J. Hazard Mater. 308, 243–252. https://doi.org/10.1016/j.jhazmat.2016.01.022.

Shin, J.H., Yu, J., Wang, L., Kim, J., Koh, S.-M., 2019. Investigation of spectral variation of pine needles as an indicator of arsenic content in soils. Minerals 9, 498. https://doi.org/10.3390/min9080498.

Slonecker, E.T., Fisher, G.B., Aiello, D.P., Haack, B., 2010. Visible and infrared remote imaging of hazardous waste: a review. Rem. Sens. 2, 2474–2508. https://doi:10.3390/rs2112474.

Verrelst, J., Muñoz, J., Alonso, L., Delegido, J., Rivera, J.P., Camps-Valls, G., Moreno, J., 2012. Machine learning regression algorithms for biophysical parameter retrieval: opportunities for Sentinel-2 and-3. Remote Sens. Environ. 118, 127–139. https://doi.org/10.1016/j.rse.2011.11.002.

Verrelst, J., Malenovský, Z., Van der Tol, C., Camps-Valls, G., Gastellu-Etchegorry, J.-P., Lewis, P., North, P., Moreno, J., 2019. Quantifying vegetation biophysical variables from imaging spectroscopy data: a review on retrieval methods. Surv. Geophys. 40, 589–629. https://doi.org/10.1007/s10712-018-9478-y.

Wang, F., Gao, J., Zha, Y., 2018. Hyperspectral sensing of heavy metals in soil and vegetation: feasibility and challenges. ISPRS J. Photogrammetry Remote Sens. 136, 73–84. https://doi.org/10.1016/j.isprsjprs.2017.12.003.

Yang, X., Lei, S., Zhao, Y., Cheng, W., 2020. Use of hyperspectral imagery to detect affected vegetation and heavy metal polluted areas: a coal mining area. China. Geocarto. International 37 (10), 2893–2912. https://doi.org/10.1080/10106049.2020.1844308.

Zarco-Tejada, P.J., Miller, J.R., Mohammed, G.H., Noland, T.L., 2000. Chlorophyll fluorescence effects on vegetation apparent reflectance: I. Leaf-level measurements and model simulation. Rem. Sens. Environ. 74, 582–595.

Zarco-Tejada, P.J., Miller, J.R., Harron, J., Hu, B., Noland, T.L., Goel, N., Mohammed, G. H., Sampson, P., 2004. Needle chlorophyll content estimation through model inversion using hyperspectral data from boreal conifer forest canopies. Rem. Sens. Environ. 89 ‘ (2), 189–199. https://doi.org/10.1016/j.rse.2002.06.002.

Zarco-Tejada, P.J., Hornero, A., Beck, P.S.A., Kattenborn, T., Kempeneers, P., Hernández-Clemente, R., 2019. Chlorophyll content estimation in an open-canopy conifer forest with Sentinel-2A and hyperspectral imagery in the context of forest decline. Rem. Sens. Environ. 223, 320–335. https://doi.org/10.1016/j.rse.2019.01.031.

Zhang, C., Ren, H., Dai, X., Qin, Q., Li, J., Zhang, T., Sun, Y., 2019. Spectral characteristics of copper-stressed vegetation leaves and further understanding of the copper stress vegetation index. Int. J. Rem. Sens. 40 (12), 4473–4488. https://doi.org/10.1080/01431161.2018.1563842.

Zhang, Y., Migliavacca, M., Penuelas, J., Ju, W., 2021. Advances in hyperspectral remote sensing of vegetation traits and functions. Remote Sens. Environ. 252 https://doi.org/10.1016/j.rse.2020.112121. ISSN 0034-4257.

Zhou, C., Chen, S., Zhang, Y., Zhao, J., Song, D., Liu, D., 2018. Evaluating Metal Effects on the Reflectance Spectra of Plant Leaves during Different Seasons in Post-Mining Areas, China. Remote Sens 10, 1211. https://doi.org/10.3390/rs10081211.